Journal of Alloys and Compounds 495 (2010) 108–112

Contents lists available at ScienceDirect

Journal of Alloys and Compounds

journal homepage: www.elsevier.com/locate/jallcom

Synthesis of submicron $BaTiO_3$ particles by modified solid-state reaction method

Che-Yuan Chang[a], Chi-Yuen Huang[a,*], Yu-Chun Wu[a], Che-Yi Su[b], Cheng-Liang Huang[b]

[a] Department of Resources Engineering, National Cheng Kung University, Tainan, Taiwan
[b] Department of Electrical Engineering, National Cheng Kung University, Tainan, Taiwan

ARTICLE INFO

Article history:
Received 7 September 2009
Received in revised form 20 January 2010
Accepted 21 January 2010
Available online 1 February 2010

Keywords:
$BaTiO_3$
Powder synthesis
Core–shell
Urea

ABSTRACT

$BaTiO_3$ powders were prepared according to a novel fabrication route. Submicrometric TiO_2 particles were coated by $BaCO_3$ nanoparticles which are precipitated by urea decomposition method. Under suitable operation conditions, homogeneous core–shell TiO_2@$BaCO_3$ structure, an optimal $BaCO_3$ precipitation yield and stoichiometry control was achieved. $BaTiO_3$ particles were successfully obtained after heat treatment at 1000 °C for 1 h. The size of the obtained particle was about 150–200 nm, in agreement with the original size of the TiO_2 core.

1. Introduction

Barium titanate ($BaTiO_3$) is a material widely applied in the electronic industries due to its high dielectric constant and low tangent losses. It is often used as a basic ferroelectric material of electronic components, such as multilayer ceramic capacitor (MLCC), positive temperature coefficient (PTC) thermistors and sensors. It is known that the number of active layers in a single capacitor of the latest MLCC type exceeds 1000, which means that each dielectric has to be less than 1 μm thick [1,2]. Practically, dielectric properties of $BaTiO_3$ depend strongly on its grain size. When its grain size in bulk body is 0.6–0.8 μm, the properties are generally optimal [3]. Accordingly, one should use $BaTiO_3$ particles of 100–200 nm as the starting material taking into account the grain growth that occurs during the sintering process [4–6]. Conventional solid-state reaction is one of the most commonly used synthetic methods for fabricating pure $BaTiO_3$ particles; however, it often requires a high calcination temperature to obtain pure $BaTiO_3$ phase and the final product is usually coarse and seriously agglomerated which fails to satisfy industrial needs. Milling treatment could be a method for deagglomeration of the $BaTiO_3$ powder obtained from solid-state reaction; however, a leach of barium ions into the aqueous suspension often occurs and results in stoichiometric problem [7]. Several chemical routes such as oxalate, sol–gel and hydrothermal methods for synthesizing fine and weakly agglomerated $BaTiO_3$ powder have been proposed; nevertheless, these methods are relatively more expensive than solid-state reaction and the particle sizes obtained are generally smaller than 100 nm [8–13]. Buscaglia et al. have synthesized $BaTiO_3$ particles by mixing $BaCO_3$ (~1 μm) with peroxy-Ti aqueous solution and obtained $BaTiO_3$ pure-phase via a calcination treatment at a temperature as low as 700 °C [14,15]. Their obtained $BaTiO_3$ particles size are around 100–200 nm with $c/a = 1.005$, however are also agglomerated. Kim et al. have prepared Mg-doped $BaTiO_3$ by coating a layer of MgO on the surface of $BaTiO_3$ and observed a homogeneous diffusion of Mg ions into the structure of $BaTiO_3$ at low temperature [16]. The present work suggests a novel and simple synthetic method for the fabrication of size-determined and dispersed $BaTiO_3$ particles. TiO_2 particles of size between 100 and 150 nm were used as the core material. $BaCO_3$ nano-coating on the TiO_2 surface was carried out by urea precipitation method under various conditions in order to acquire an optimal yield of $BaCO_3$. Nanoparticles pure-phase $BaTiO_3$ single crystals of size around 120–150 nm were obtained after heating at 1000 °C for 1 h.

2. Experimental details

Rutile TiO_2 powder (TiO_2 99.9%, SSA = 10 m^2/g) of high quality, barium nitrate ($Ba(NO_3)_2$, 99%, Acros), and urea (NH_2CONH_2, >99.5%, Merck) were used as the starting materials. The as-received TiO_2 powder was milled for 4 h in deionized water by yttrium-stabilized tetragonal zirconia polycrystals (Y-TZP) grinding balls (ϕ = 2 mm). The mean size of the as-milled TiO_2 particle was 100–150 nm. Urea and $Ba(NO_3)_2$ aqueous solution was prepared with various [urea]/[Ba^{2+}] atomic ratio (labeled R) from 5 to 40. The as-prepared [urea]/[Ba^{2+}] solution was stoichiometrically added into the TiO_2 suspension at a feeding rate of 2.5 ml/min. The mixture was vigorously stirred at 90 °C for various durations (labeled t) ranging from 8 to 48 h. The precipitate was collected by filtration with a membrane filter (0.1 μm, Advantec) to remove the unreached substances. The precipitate was dried in a box furnace at 100 °C for 24 h and then heat treated from 700 to 1000 °C for

* Corresponding author. Tel.: +886 6 2754170; fax: +886 6 2380421.
E-mail address: cyhuang@mail.ncku.edu.tw (C.-Y. Huang).

0925-8388/$ – see front matter © 2010 Elsevier B.V. All rights reserved.
doi:10.1016/j.jallcom.2010.01.096

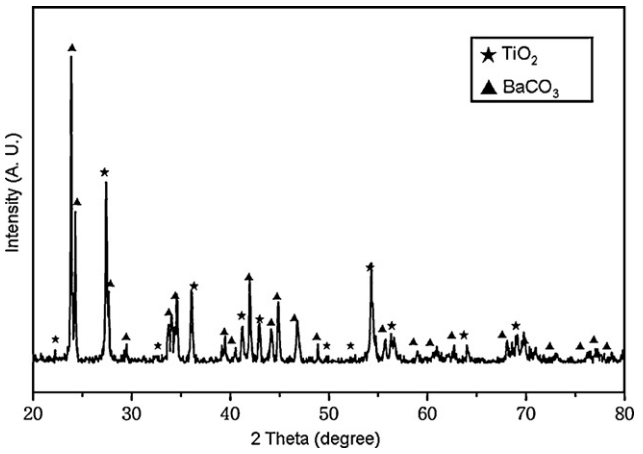

Fig. 1. XRD pattern of the as-obtained dried powder as the $R = 30$ and reacts at 90 °C for 36 h.

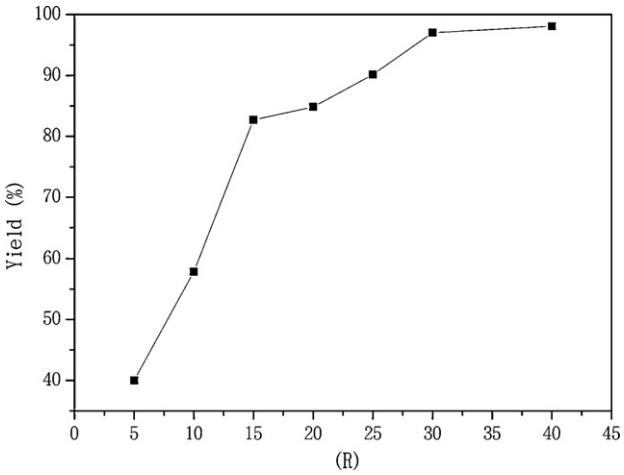

Fig. 3. Yield of precipitation as a function of R under 90 °C for 24 h reaction condition.

1 h, respectively. Fourier transformation infrared spectroscopy (FTIR, EQUINOX 55, Bruker-AXS) was employed to characterize the chemical compositions. Structural properties were studied by X-ray diffraction (XRD, D5000, Siemens) and transmission electron microscope (TEM, Tecnai G^2 F20, FEI). The particle size distribution of $BaTiO_3$ powder was confirmed by Laser Diffraction Particle Size Analyzer (90 Plus/Bi-MAS, Brookhaven) and the ethanol was used as the dispersant during the measurement.

3. Results and discussion

It is known that hydrolysis of urea in water gives rise to a formation of ammonia and carbon dioxide according to the following reaction [17–19]:

$$(H_2N)_2CO + 3H_2O \xrightarrow{\Delta} CO_2 + 2NH_3 + 2H_2O$$

The dissolved CO_3^{2-} in water induces a reaction with Ba^{2+} ions liberated from $Ba(NO_3)_2$ and forms $BaCO_3$ precipitates, which are gradually deposited on the surface of TiO_2 particles. XRD pattern of the as-dried precipitates, as presented in Fig. 1, shows clearly two crystallized phases which are TiO_2 rutile (ICDD-PDF# 75-1748) and $BaCO_3$ (ICDD-PDF# 71-2394), respectively. FTIR analysis was also employed to verify if there are any non-crystalline phases coexisting in the as-obtained precipitate which were not possible to be detected by XRD. FTIR spectrum of the as-dried precipitates is illustrated in Fig. 2(a). High purity rutile TiO_2 and pure commercial $BaCO_3$ powders were also measured as reference spectra shown in Fig. 2(b) and (c), respectively. It is found that the absorption bands corresponding to Fig. 2(a) are in fair agreement with the combination of rutile TiO_2 and pure $BaCO_3$ where no absorption bands other than these two phases were observed. It reconfirms that $BaCO_3$ is the only product during the urea precipitation process.

It is worthy of mentioning that the reaction rate of $BaCO_3$ precipitation in the present method has to be slow enough in order to obtain a homogeneous core–shell structure; otherwise the rapid precipitation may produce a phase separation between $BaCO_3$ and TiO_2 which is unfavorable for $BaTiO_3$ formation. The precipitation process was held at 90 °C, at which the reaction rate is found to be appropriate [20]. Moreover, the yield of $BaCO_3$ has to be also carefully controlled to maintain a correct [Ba/Ti] stoichiometry. It has been reported that urea-excess environment helps to enhance the yield of product from the urea precipitation method [21–23]. Accordingly, reactions with various R were conducted in order to explore an optimal urea ratio related to the yield of $BaCO_3$ precipitation. The yield of $BaCO_3$ precipitation was calculated according to the following relation:

$$\frac{(W_d - W_{TiO_2})/M_{BaCO_3}}{W_{Ba(NO_3)_2}/M_{Ba(NO_3)_2}} \times 100\%$$

where W_d is the total weight of the dried precipitates; $W_{Ba(NO_3)_2}$ and W_{TiO_2} are the weights of the starting TiO_2 and $Ba(NO_3)_2$ pow-

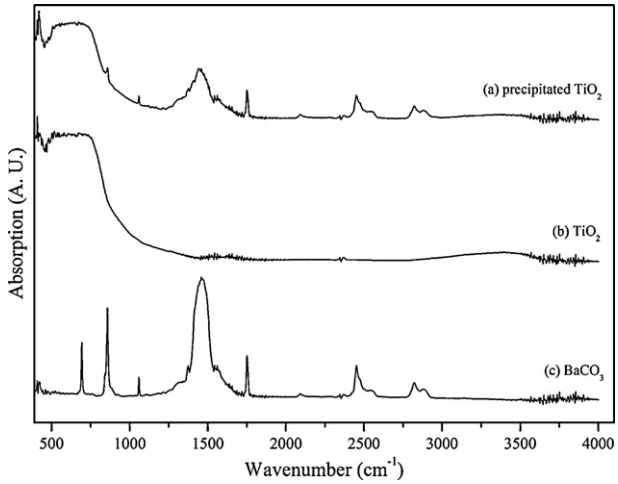

Fig. 2. FTIR spectra of the precipitation powder as the $R = 30$ and reacts at 90°C for 36 h. (a) precipitated TiO_2, (b) rutile TiO_2 and (c) $BaCO_3$.

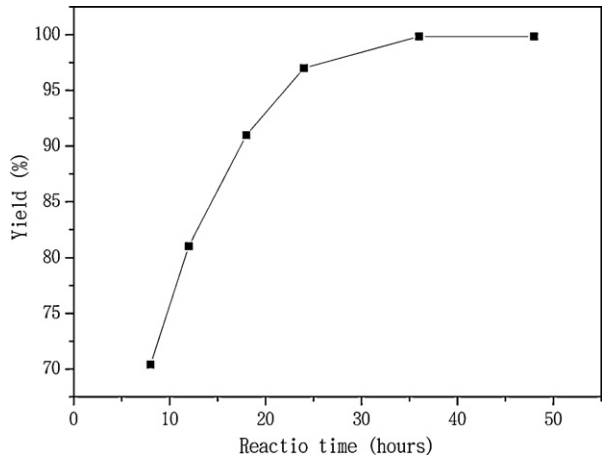

Fig. 4. Yield of precipitation as a function of reaction time as the $R = 30$ and reaction temperature is 90 °C.

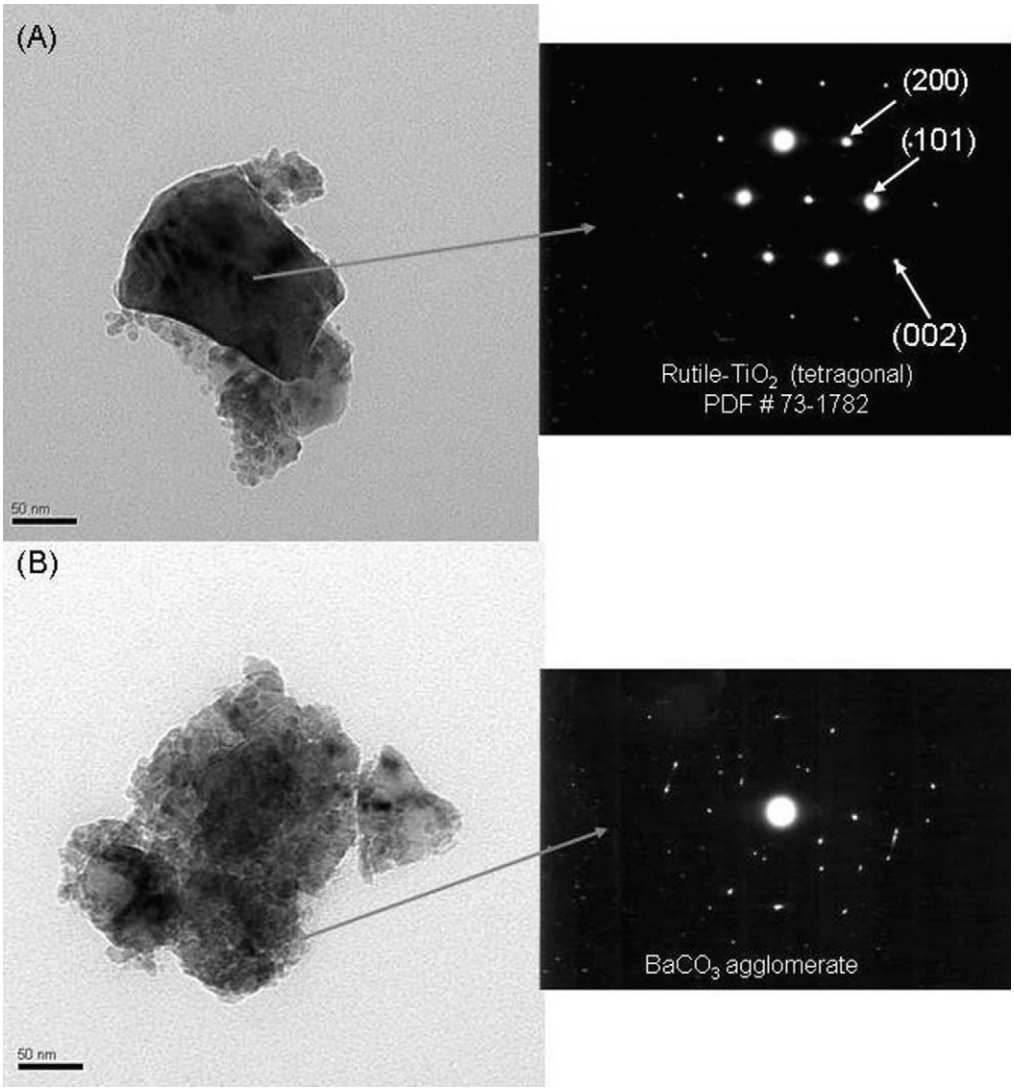

Fig. 5. Morphology (TEM) and diffraction patterns of the precipitation powder. (A) $R = 5$, (B) $R = 30$ reacts at 90 °C for 36 h.

der, respectively. M_{BaCO_3} and $M_{Ba(NO_3)_2}$ are the molecular weights of $BaCO_3$ and $Ba(NO_3)_2$, respectively. As a result, the yield of $BaCO_3$ as a function of R reacting at 90 °C for 24 h is presented in Fig. 3. It is found that the yield increases rapidly from 40% to 82% when R increases from 5 to 15. The increasing rate of yield is relatively slower as R exceeds 15 and tends to stabilize when R exceeds 30. Since the yield does not show an obvious enhancement between $R = 30$ and 40, the former is thus selected as the experimental condition for the following work. On the other hand, the yield of $BaCO_3$ precipitation is also dependent on the reacting duration especially when the reaction rate in the present method is quite slow. The yield obtained under the condition of $R = 30$ as a function of reaction time (t) at 90 °C is presented in Fig. 4. One can see that the yield increases with reaction time until holding for 36 h. As a consequence, the experimental parameters for obtaining a good yield of $BaCO_3$ are thus set as $R = 30$ and $t = 36$ h.

To investigate the morphology of the products obtained under different experimental conditions, the precipitates reacted at $R = 5$ and $R = 30$ at 90 °C for 36 h were observed by TEM and are shown in Fig. 5. According to the electron diffraction patterns shown in the insets of Fig. 5, the large and small particles are assigned to single crystal of TiO_2 and polycrystalline of $BaCO_3$, respectively. Under the condition of $R = 5$, the large TiO_2 particle is only partially covered by $BaCO_3$ nanoparticles due to insufficient production yield. Nevertheless, a core–shell structure is effectively formed for $R = 30$ where the TiO_2 core particle is entirely enclosed by $BaCO_3$ nanocrystallites with a homogeneous thickness of around 50 nm as shown in Fig. 5(B).

XRD patterns of the dried precipitates prepared at $R = 30$ and $t = 36$ h and annealed at temperatures from 700 to 1000 °C for 1 h are presented in Fig. 6. The peak at around 31.6° corresponding to the diffraction peaks of (1 0 1) and (1 1 0) of $BaTiO_3$, starts to appear after heating at 700 °C for 1 h. The amount of $BaTiO_3$ slightly increases when heated at 800 °C while $BaCO_3$ and TiO_2 still remain. An intermediate phase of Ba_2TiO_4 is emerges after heating at 900 °C and $BaCO_3$ is completely disappears in the meantime. Pure $BaTiO_3$ is finally obtained at 1000 °C.

According to the XRD analysis, the reactions that occur between $BaCO_3$ and TiO_2 can be stated by the following steps:

$$BaCO_3 + TiO_2 \rightarrow BaTiO_3 + CO_2 \quad (1)$$

$$BaCO_3 + BaTiO_3 \rightarrow Ba_2TiO_4 + CO_2 \quad (2)$$

$$2BaCO_3 + TiO_2 \rightarrow Ba_2TiO_4 + 2CO_2 \quad (3)$$

$$Ba_2TiO_4 + TiO_2 \rightarrow 2BaTiO_3 \quad (4)$$

The reaction as expressed in Eq. (1) is occurred at around 700–800 °C that should take place at the core/shell boundary and

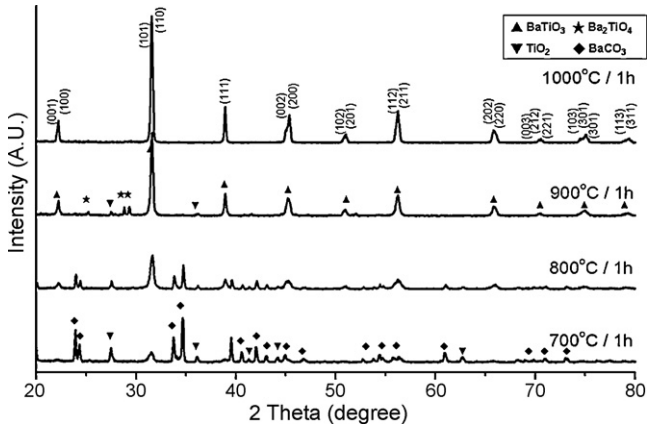

Fig. 6. XRD pattern of the precipitation powder calcined at various temperatures.

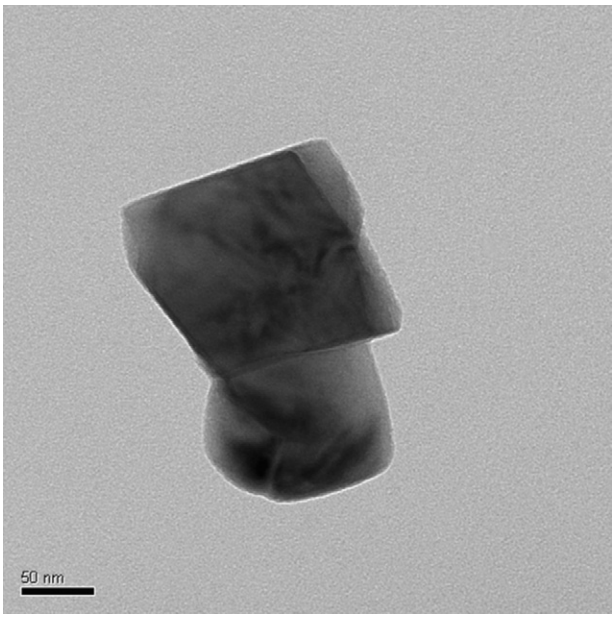

Fig. 7. Morphology (TEM) of the as-calcined $BaTiO_3$ powder (1000 °C/1 h calcination).

forms a fraction of $BaTiO_3$. In this stage, $BaCO_3$ and TiO_2 are still the major phases in the system. As the temperature rises up to 900 °C, the mobility of Ba^{2+} becomes higher that drives Ba^{2+} ions diffusing into the as-formed $BaTiO_3$ lattice and forms Ba_2TiO_4 as described in Eq. (2). In the meantime, $BaCO_3$ may also react with the remaining TiO_2 to form Ba_2TiO_4 as expressed in Eq. (3) because a slight decrease in TiO_2 is observed between 800 and 900 °C. Finally, the intermediate Ba_2TiO_4 phase interacts with the rest of TiO_2 and transforms into a stable $BaTiO_3$ phase at 1000 °C as expressed in Eq. (4).

According to the present method, the size of the core–shell structure is mainly determined by the size of TiO_2 particles. Since the [Ba/Ti] atomic ratio is controlled at 1, the volumetric ratio between $BaCO_3$ and TiO_2 is 2.36 according to their theoretical densities ($D_{BaCO_3} = 4.43 g/cm^3$ and $D_{TiO_2} = 4.23 g/cm^3$) and molecular weights ($W_{BaCO_3} = 197.3 g/mole$ and $W_{TiO_2} = 79.88 g/mole$). A relation correlating the core size with the shell thickness can be generally expressed as Eq. (5)

$$\frac{4/3\pi(X+Y)^3 - 4/3\pi(X)^3}{4/3\pi(X)^3} = 2.36 \quad (5)$$

where X is the radius of TiO_2 particle and Y is the thickness of the $BaCO_3$ layer. In the present work, TiO_2 core particles are of size 100–150 nm. For the example of TiO2 particle of 100 nm ($X = 50$) as illustrated in Fig. 5(B), the theoretical shell thickness (Y) of $BaCO_3$ derived from Eq. (5) is 24.8 nm. The diameter of total core–shell structure is theoretically 149.7 nm, which is consistent with the TEM observation. Pure $BaTiO_3$ particles derived from the reaction of TiO_2 and $BaCO_3$ generate a volumetric reduction of around 60.4% due to the difference in bulk density ($D_{BaTiO_3} = 6.08 g/cm^3$), which is equivalent to a reduction in particle diameter of 84.5%. For the example of a core–shell grain of 149.7 nm, the resulting $BaTiO_3$ particles should be 126.4 nm. The single crystal of $BaTiO_3$ fabricated by the present method shows a particle size of 150–200 nm, as illustrated in Fig. 7, which is in agreement with the as-obtained core–shell structure as shown in Fig. 5(B). In comparison with the conventional solid-state reaction, the present method decreases effectively the calcining temperature for obtaining pure $BaTiO_3$ phase and the crystal size is also controlled at submicron scale of 150–200 nm. The size distribution of the $BaTiO_3$ prepared by the present method was measured by laser scattering method and is shown Fig. 8. It is found that the powder is generally monodispersed at around 560 nm, and a fraction at around 420 nm. In comparison with TEM observation shown above, the primary particles of $BaTiO_3$ are around 150–200 nm. It means the obtained particle is slightly

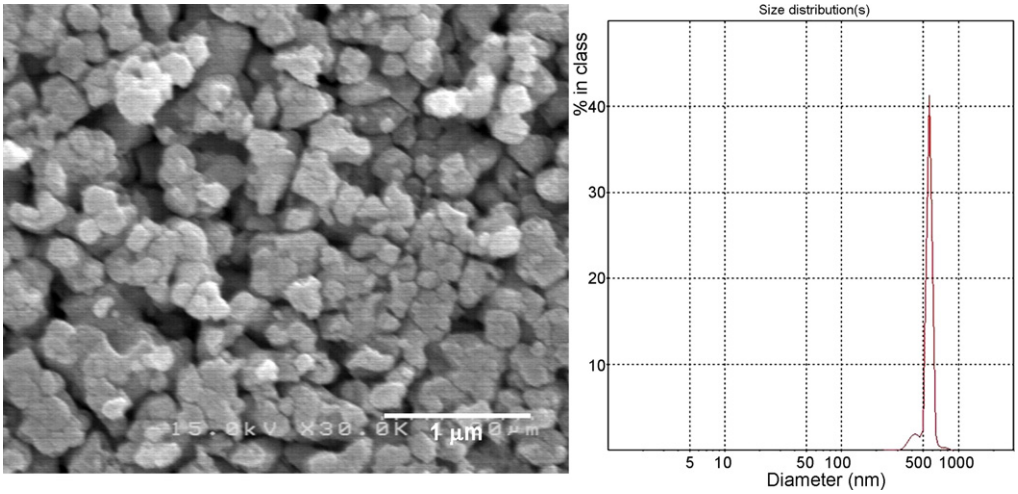

Fig. 8. Morphology (SEM) and particle size distribution of the as-calcined $BaTiO_3$ powder (1000 °C/1 h calcination).

aggregated. Nevertheless, the agglomeration drawbacks occur for other synthesis methods are obviously improved.

4. Conclusions

This study describes a modified solid-state reaction process for the synthesis of submicron $BaTiO_3$ particles. Urea and $Ba(NO_3)_2$ are used as the starting materials to produce precipitates of nano-sized $BaCO_3$ coated onto the TiO_2 surface, forming a core–shell structure. Atomic ratio of [urea]/[Ba^{2+}] = 30 and reaction time = 36 h are optimal conditions for obtaining a good yield of $BaCO_3$ precipitation and allow the stoichiometry of [Ba/Ti] to be controlled at 1. Submicrometric and dispersed $BaTiO_3$ particles are obtained by a brief heat treatment at 1000 °C for 1 h.

References

[1] C. Pithan, D. Hennings, R. Waser, Int. J. Appl. Ceram. Technol. 2 (1) (2005) 1.
[2] C.C. Lin, W.C.J. Wei, C.Y. Su, C.H. Hsueh, J. Alloys Compd. 485 (2009) 653–659.
[3] A.V. Polotai, A.V. Ragulya, C.A. Randall, Ferroelectric 288 (2003) 93.
[4] D.F.K. Hennings, B.S. Schreinemacher, H. Schreinemacher, J. Am. Ceram. Soc. 84 (12) (2001) 2777.
[5] S.S. Ryu, D.H. Yoon, J. Mater. Res. 42 (2007) 7093–7099.
[6] W. Wei, G. Xu, Z. Ren, G. Shen, G. Han, J. Am. Ceram. Soc. 91 (11) (2008) 3774–3780.
[7] A.J. Moulson, J.M. Herbert, Electroceramics: Materials, Properties and Applications, second ed., John Wiley and Sons, New York, 2003.
[8] Y. Xie, S. Yin, T. Hashimoto, Y. Tokano, A. Sasaki, T. Sato, J. Eur. Ceram. Soc. 30 (2010) 699–704.
[9] L.Q. Wang, L. Liu, D.F. Xue, H.G. Kang, G.H. Liu, J. Alloys Compd. 440 (2007) 78–83.
[10] J.H. Kim, W.S. Jung, H.T. Kim, D.K. Yoon, Ceram. Int. 35 (2009) 2337–2342.
[11] W. Li, Z.J. Xu, R.Q. Chu, P. Fu, J.G. Hao, J. Alloys Compd. 482 (2009) 137–140.
[12] V.V. Sydorchuk, V.A. Zazhigalov, S.V. Khalameida, K.W. Ciurowa, J.S. Ziba, R. Leboda, J. Alloys Compd. 482 (2009) 229–234.
[13] C. Ando, R. Yanagawa, H. Chazono, H. Kishi, M. Senna, J. Mater. Res. 19 (12) (2004) 3592.
[14] M.T. Buscaglia, M. Bassoli, V. Buscaglia, J. Am. Ceram. Soc. 88 (9) (2005) 2374.
[15] M.T. Buscaglia1, V. Buscaglia, M. Viviani1, G. Dondero, S. Röhrig, A. Rüdiger, P. Nanni, Nanotechnology 19 (22) (2008) 225602.
[16] J.N. Kim, T.S. Byun, C.S. Kim, J. Chem. Eng. Japan 38 (8) (2005) 553.
[17] I. Sondi, E. Matijevic, Chem. Mater. 15 (2003) 1322.
[18] C. Beddie, C.E. Webster, M.B. Hall, Roy. Soc. Chem. (2005) 3542.
[19] F. Boschini, B. Robertz, A. Rulmont, R. Cloots, Eur. Ceram. Soc. 23 (2003) 3035.
[20] L.W. Diamond, N.N. Akinfiev, Fluid Phase Equilibr. 208 (2003) 265.
[21] H. Ichinose, M. Terasaki, H. Katsuki, J. Sol–Gel Sci. Technol. 22 (2001) 33.
[22] Y. Gao, Y. Masuda, Z. Peng, T. Yonezawa, K. Koumoto, J. Mater. Chem. 13 (2003) 608.
[23] W. Lu, M. Quilitz, H. Schmidt, J. Eur. Ceram. Soc. 27 (10) (2006) 3149.